Accepted Manuscript

A water-soluble "turn-on" fluorescent probe for specifically imaging mitochondria viscosity in living cells

Hui Wang, Bin Fang, Lufei Xiao, Di Li, Le Zhou, Lin Kong, Yan Yu, Xiangzi Li, Yunjun Wu, Zhangjun Hu

PII:	S1386-1425(18)30521-3
DOI:	doi:10.1016/j.saa.2018.05.121
Reference:	SAA 16155
To appear in:	*Spectrochimica Acta Part A: Molecular and Biomolecular Spectroscopy*
Received date:	2 April 2018
Revised date:	27 May 2018
Accepted date:	29 May 2018

Please cite this article as: Hui Wang, Bin Fang, Lufei Xiao, Di Li, Le Zhou, Lin Kong, Yan Yu, Xiangzi Li, Yunjun Wu, Zhangjun Hu , A water-soluble "turn-on" fluorescent probe for specifically imaging mitochondria viscosity in living cells. Saa (2017), doi:10.1016/j.saa.2018.05.121

A water-soluble "turn-on" fluorescent probe for specifically imaging mitochondria viscosity in living cells

Hui Wang[a,*,†], Bin Fang[b,†], Lufei Xiao[c,*], Di Li[a], Le Zhou[a], Lin Kong [b], Yan Yu[a], Xiangzi Li[a], Yunjun Wu[a], Zhangjun Hu[d]

[a] Department of Chemistry, Anhui provincial engineering research center for polysaccharide drugs, Wannan Medical College, Wuhu 241002, People's Republic of China

[b]Department of Chemistry, Key Laboratory of Functional Inorganic Material Chemistry of Anhui Province, Anhui University, Hefei 230601, P. R. China

[c] Department of Food and Environmental Engineering, Chuzhou Vocational and Technical college, Chuzhou 239000, P. R. China;

[d] Division of Molecular Surface Physics & Nanoscience, Department of Physics, Chemistry and biology (IFM), Linköping University, 58183, Linköping, Sweden

E-mail address: wanghias@126.com; xlf3345@163.com

† These authors contributed equally to this work and should be considered co-first authors.

Abstract

Rational design of water-soluble probes for mitochondrial viscosity in practical biological applications remains a challenge. Herein, we described a novel hydro soluble benzothiazole salt derivative **MitoSN**, which exhibits specifically response and singular sensitivity to the mitochondria viscosity in living Hela cells. **MitoSN** displays an excellent fluorescence enhancement (ca. 35-fold) with the increase of the viscosity in the water-glycerol system. Moreover, confocal microscopy indicates that **MitoSN** is sensitive to the local viscosity and selectively stains mitochondria, the body of zebrafish as well. Importantly, **MitoSN** is capable to identify the viscosity difference of mitochondria in normal and nystatin treated Hela cells. The work

provides a useful tool to monitor the changes of viscosity in the mitochondrial microenvironment.

Keywords: water-soluble; mitochondrial targeting; viscosity sensing; benzothiazole salt; zebrafish

1. Introduction

Intracellular viscosity plays an important part in the process of cellular diffusion, including bio-macromolecular interactions and diffusion of reactive metabolites [1-5]. Abnormal changes in the viscosity at cellular level accompany with a number of diseases and malfunctions, such as atherosclerosis and Alzheimer's disease [6]. Moreover, at the sub-organelle levels, mitochondrial viscosity could influence the signaling interactions of chemicals and biomolecules. The abnormal viscosity in the mitochondrial matrix could induce the change of mitochondrial network organization and further influence metabolite diffusion, which is related to many diseases and malfunctions in cellular aspects [7-8]. For instances, Lin et al. presented two new mitochondrial-targeted fluorescent viscosity probes [9]. Very recently, Lin's group reported a ratiometric two-photon fluorescent probe to monitor the changes of mitochondrial viscosity [10]. Tian and co-workers developed a water-soluble two-photon fluorescence sensor, which is specifically responsive to the mitochondrial viscosity in living cells [11]. Thus, it is significant to rationally design and synthesize mitochondrial-targeted probes to monitor intracellular mitochondrial viscosity at subcellular level.

In recent years, molecular rotor has been regarded as a sort of typical fluorophore, in which the fluorescence relies on the rate of intramolecular rotation. In non-viscous media, the probe coupled with a rotor moiety can give rise to a weak intrinsic fluorescence, whereas in viscous media, the inhibited rotation reduces the probability of non-radiative pathways and subsequently restores the fluorescence [12-17]. Therefore, such biocompatible molecular fluorophores containing molecular rotors are potentially used as viscosity-sensitive fluorescent chemosensors in biosystem.

In this work, a water-soluble molecule (**MitoSN**) with a rotor unit was designed and synthesized (**Scheme 1**). Firstly, ethyl acetate group contributes the lipid solubility and biocompatibility. Secondly, benzothiazole is an electron-withdrawing building block with high photophysical stability. Thirdly, the benzothiazole cation moiety not only works as targeting mitochondria moiety, but enhances the water-solubility of the resulted MitoSN. As expected, **MitoSN** exhibits excellent solubility and low cytotoxicity. The cellular studies demonstrate that **MistoSN** is able to target mitochondria and exhibit obvious enhanced fluorescent response to mitochondrial viscosity. Therefore, the "turn-on" fluorescent probe for mitochondrial viscosity is achieved.

2. Experiments

2.1. Materials and apparatus

All chemicals were purchased as reagent grade and used without further purification. The products were performed with a PerkineElmer 240 analyzer. IR spectra (4000-400 cm^{-1}), in KBr pressed pellets, were obtained on a Nicolet FT-IR-870SX spectrophotometer. The ^{1}H NMR and ^{13}C NMR spectra were recorded on at 25 ℃ using Bruker 400 Ultrashield spectrometer. Mass spectrum was recorded on HRMS-LTQ Obritrap XL (ESI source).The UV-*vis* absorption spectra were measured on a UV-1700 spectrophotomter. The one-photon excited fluorescence spectra measurements were measured on Hitachi F-4600 fluorescence spectrophotometer.

The fluorescence quantum yields (Φ) were determined by using fluorescein as the reference according to the literature method [18].

2.2 Synthetic of MitoSN

Preparation of M

2-Methylbenzothiazole (1.49 g, 10 mmol) and ethyl 2-bromoacetate (1.67 g, 10 mmol) were mixed in 50 mL toluene. The solutions was refluxed for 24 h, then the precipitate produced was filtered, washed with toluene and fried *in vacuo* to obtain

white solid. Yield: 90%. ^{1}H NMR (D_2O,400 MHz) δ: 8.07 (d, J = 8.0 Hz, 1H), 7.90 (d, J = 8.6 Hz, 1 H), 7.73 (d, J = 7.7 Hz, 1 H), 7.68 (m, 1 H), 5.58 (s, 2 H), 4.70 (s, 2 H), 4.19 (q, J = 7.2 Hz, 2 H), 3.05 (m, 1 H), 1.16 (t, J = 7.2 Hz, 3 H).

Preparation of MitoSN

Using a 100 mL one-necked flask fitted with a stirrer and a condenser, 3.26 g (10 mmol) of **M**, 1.22 g (10 mmol) of p-Hydroxybenzaldehyde and 30 mL of absolute ethanol were mixed. Three drops of piperidine were added to the solutions and refluxed for 24 h. After cooling, the solution was filtered, and washed thrice with ether. Yellow solid product **MitoSN** was collected. Yield: 87 %. IR (KBr, cm^{-1}) selected bands: 3083, 2927, 1743, 1583, 1517, 1443, 1485, 1443, 1395, 1339, 1298, 1273, 1214, 1170, 1050, 966, 828, 764, 635, 512, 490. ^{1}H NMR (400 MHz, d_6-DMSO) δ : 10.71 (s, 1 H), 8.44 (d, J = 7.9 Hz, 1 H), 8.27 (d, J = 15.5 Hz, 1 H), 8.15 (d, J = 8.4 Hz, 1 H), 7.97 (d, J = 8.7 Hz, 2 H), 7.90 (m, 3 H), 6.96 (d, J = 8.7 Hz, 2 H), 6.01 (s, 2 H), 4.25 (q, J = 7.1 Hz, 2 H), 1.25 (t, J = 7.1 Hz, 3 H). ^{13}C NMR (100 MHz, d_6-DMSO) δ: 173.9, 165.7, 162.6, 151.1, 141.1, 133.0, 129.5, 128.2, 126.9, 125.3, 124.4, 116.3, 109.4, 62.4, 49.2, 13.9. *m/z* : 340.09 ($[M]^+$).

3. Results and Discussions

3.1 Synthesis and spectral properties of MitoSN

The synthetic process of **MitoSN** was presented in **Scheme 2**. It can be easily synthesized in two steps. **MitoSN** was fully characterized by ^{1}H NMR, ^{13}C NMR, ESI-MS and IR spectra (ESI, **Fig S1-S4**). UV-vis absorption spectra of **MitoSN** in different solvents were studied (**Table S1**). As shown in **Fig S5**, the absorption band of **MitoSN** exhibits one band between 350 and 500 nm, which could be assigned to the intramolecular charge transfer (ICT) mixed with π-π* transition, as confirmed by TD-DFT calculations (**Fig S6** and **Table S2**). The fluorescence emission peak of **MitoSN** around 520 nm was observed when excited at 420 nm. The fluorescence quantum yields of **MitoSN** are quite low in these solvents (**Table S1**), which is favor of the bioimaging application due to its low background fluorescence. Moreover, a weak solvatochromism was observed with the increasing solvent polarities, which is

very important to the molecular rotor for sensing the intracellular viscosity [19-21]. Furthermore, the water solubility were also studied *via* UV-vis absorption spectra. As displayed in **Fig S7**, the absorbance is linear to the concentration in the region of 10-100 μM, revealing **MitoSN** possessed good water solubility (100 μM), which is a significant advantage for biological application.

3.2 Response to viscosity by the naked eye

The viscosity-sensitive response of **MitoSN** was performed and presented in **Fig 1**. **MitoSN** exhibited weak fluorescence and low quantum yields (QY < 0.01) in non-viscous solution. In stark contrast, in high viscous solutions, a strong emission peak at 530 nm was obviously observed (**Fig 1a**). The fluorescence intensity of **MitoSN** enhanced about 35-fold (QY = 0.10) with the viscosity of the solutions increasing from 1.0 cP (water) to approximately 950 cP (99% glycerol). Moreover, the obvious "turn-on" fluorescence response of **MitoSN** could be observed by the naked eye (inset of **Fig 1a**). In addition, a better linear relationship (R^2 = 0.992, the slope x = 0.495) was obtained between the logarithm of the fluorescence intensity ratio ($\log(I/I_0)$) and the logarithm of the viscosity ($\log \eta$). These results revealed that **MitoSN** could be worked as fluorescent probe to quantitatively detect the environmental viscosity.

The mechanism of the light-switch effect of **MitoSN** can be explained by the molecular rotor effect [22-23]. In non-viscous solution, **MitoSN** was non-emissive due to that the free rotation of the vinyl bond induced a non-radiative process, resulting in quenched fluorescence. However, in the viscous solutions, the rotation is restricted, restoring the fluorescence enhancement [24-25]. Besides, the rotor mechanism was further evidenced by the absorption spectra. As depicted in **Fig S8**, an obvious red-shift was clearly observed from 418 nm to 433 nm, suggesting probe **MitoSN** might take more plane shape to extend the degree of conjugation in viscous media compared to non-viscous media.

3.3. Biological imaging application

To further investigate the potential application of probe **MitoSN** in biological imaging, the cytotoxicity test was firstly evaluated by MTT assay. As shown in **Fig S9,** after over 24 hours of incubation with probe **MitoSN**, high cell viability was obtained at the concentrations between 5 μM and 25 μM. The results elucidated that **MitoSN** in such concentration range exhibits low toxicity in living cells.

Cell-staining experiment was carried out under confocal microscopy. As displayed in **Fig 2**, **MitoSN** could penetrate the cell cytosol within a short incubation period (30 min) and exhibited intense luminescence. To demonstrate the intracellular localization of probe **MitoSN**, co-staining experiments within Mitotracker deep red (MTDR) were performed. The fluorescence of probe **MitoSN** overlapped well with that of MTDR at a Pearson's coefficient Rr = 0.92 (**Fig 2a** and **2b**). **Fig 2c** showed that the intensity profiles of probe **MitoSN** and MTDR are nearly overlapping, which indicated that probe **MitoSN** precisely targeted mitochondria in live cells.

Mitochondrial membrane potential (ΔΨm) is an important parameter related to mitochondrial metabolic function [26]. CCCP, one of the representatives uncouples for mitochondria-related pathology and pharmacology was chosen to examine whether ΔΨm could influence the fluorescence signals of **MitoSN**. As shown in **Fig 3**, after treatment with CCCP, the fluorescence intensity of **MitoSN** exhibited distinct weakening, which implied that **MitoSN** was localized in mitochondria that may be membrane potential dependent.

Comparing to the relatively aqueous cytoplasm, mitochondrial matrix with various fundamental materials possesses higher viscosity, including DNA, enzymes, ribosomes, and nucleotide cofactors. To investigate the potential application of probe **MitoSN** as a mitochondrial-viscosity probe, confocal imaging was performed. Hela cells were pretreated with nystatin, a well-known ionophore which could induce mitochondrial viscosity alterations [24], and then incubated with probe **MitoSN**, **Fig 3** indicated that the fluorescence of **MitoSN** increased after treatment with nystatin. The results indicated that **MitoSN** possessed an appropriate mitochondrial targeting ability, which is in accord with mitochondrial membrane potential and it can be applied to detect abnormal mitochondrial-viscosity changes induced by nystatin.

Encouraged by the above results, we further explored the capability of **MitoSN** for mapping microviscosity *in vivo*. A five-day-old zebrafish was exposed to 10 μM **MitoSN** at different time. As displayed in **Fig 4a**, when a three-day-old zebrafish was prepared with **MitoSN** for 20 min, a bright green fluorescence was detected. Moreover, the merge images revealed that the bright fluorescence was distributed over almost the whole body of the zebrafish. After 1 hour, a significant luminescence was observed in the liver and the whole body (**Fig 4b**). Moreover, the fluorescent probe **MitoSN** was primarily on the liver of the zerafish after 2 hours (**Fig 4c**). We hypothesized that the probe **MitoSN** might slowly be transferred to the liver, and the probe may eventually be metabolized by the liver. These results revealed that **MitoSN** could act as a potential candidate to visualize the micro-viscosity *in vivo*.

4. Conclusions

In summary, a novel water-soluble **MitoSN** as a fluorescent viscosity probe was developed. **MitoSN** exhibits a remarkable turn-on" fluorescent response (ca. 35-fold enhancement) towards the increasing viscosity in the water-glycerol system. Cellular studies demonstrated that **MitoSN** was capable of imaging intracellular mitochondria viscosity. Furthermore, **MitoSN** was also successfully employed to visualize the microviscosity of live zebrafish larva *in vivo*. The valuable findings related to the rational design in this work could be a useful source to develop new mitochondrial-targeting viscosity probes for the mitochondria microenvironment.

Acknowledgements

This work was supported by grants from the Doctoral Startup Foundation of Wannan Medical College (wYRCQD201715), Natural Science Foundation of Anhui Province (1508085SMB208). The Science Foundation of Department Education of Anhui Province (KJ2017ZD49), and the Talent Foundation of the Education Department of Anhui (gxbjZD2016111).

References:

[1] Y. Baek, S. J. Park, X. Zhou, G. Kim, H. M. Kim, J. Yoon. Biosens. Bioelectron., 86 (2016) 885-891.

[2] P. Ning, P. Y. Dong, Q. Geng, L. Bai, Y. Q. Ding, X. H. Tian, R. Shao, L. Li, X. M. Meng. J. Mater. Chem. B., 5 (2017) 2743-2749.

[3] D. D. Li, X. H. Tian, A. D. Wang, L. J. Guan, J. Zheng, F. Li, S. L. Li, H. P. Zhou, J. Y. Wu, Y. P. Tian. Chem. Sci., 3 (2016) 2257-2263.

[4] M. G. Ren, B. B. Deng, K. Zhou, X. Q. Kong, J. Y. Wang, W. Y. Lin. Anal. Chem., 89 (2017) 552-555.

[5] P. S. Sherin, I. Lopez-Duarte, M. R. Dent, M. Kubankova, A. Vysniauskas, J. A. Bull, E. S. Reshetnikova, A. S. Klymchenko, Y. P. Tsentalovich, M. K. Kuimov. Chem. Sci., 8 (2017) 3523-3528.

[6] G. Bosman, I. G. P. Bartholomeus, W. J. De Grip. Gerontology., 37 (1991) 95-112.

[7] Deliconstantinos, George, V. Villiotou, J. C. Stavrides. Biochemical. Pharmacology., 49 (1995)1589-1600.

[8] S. J. Singer, G. L. Nicolson. Science., 175 (1972) 720-731.

[9] K. Zhou, M. G. Ren, B. B. Deng, W. Y. Lin. New. J. Chem., 41 (2017) 11507-11511.

[10] M. G. Ren, K. Zhou, L. Wang, K. Y. Liu, W. Y. Lin. Sens Actuat B., 262 (2018) 452-459.

[11] M. Zhao, Y. Z. Zhu, J. Su, Q. Geng, X. H. Tian, J. Zhang, H. P. Zhou, S.Y. Zhang, J. Y. Wu, Y. P. Tian. J. Mater. Chem. B., 35 (2016) 5907-5912.

[12] X. Dai, B. L. Dong, M. G. Ren, W. Y. Lin. J. Mater. Chem. B., 6 (2018) 381-385.

[13] X. Song, N. Li, C. Wang, Y. Xiao. J. Mater. Chem. B., 5 (2017) 360-368.

[14] M. H. Lee, N. Park, C. Yi, J. H. Han, J. H. Hong, K. P. Kim, D. H. Kang, J. L. Sessler, C. Kang, J. S. Kim. J. Am. Chem. Soc., 136 (2014)14136-14142.

[15] A. C. Benniston, A. Harriman, V. L. Whittle, M. Zelzer. Eur. J. Org. Chem., 3 (2010) 523-530.

[16] J. Sutharsan, D. Lichlyter, N. E. Wright, M. Dakanali, M. A. Haidekker, E. A. Theodorakis. Tetrahedron., 66 (2010) 2582-2588.

[17] X. D. Yin, Y. J. Li, Y. L. Zhu, X. Jing, Y. L. Li, D. B. Zhu. Dalton. Trans., 39 (2010) 9929-9935.

[18] X. D. Yin, Y. J. Li, Y. L. Zhu, X. Jing, Y. L. Li, D. B. Zhu. Dalton. Trans., 41 (2010) 9929-9935.

[19] D. Miguel, S. P. Morcillo, A. Martin-Lasanta, N. Fuentes, L. Martinez-Fernandez, I. Corral, M. J. Ruedas-Rama, D. J. Cardenas, L. A. D. Cienfuegos, A. Orte, J. M. Cuerva. Org. lett., 17 (2015) 2844-2847.

[20] M. A. Haidekker, T. P. Brady, D. Lichlyter, E. A. Theodorakis. J. Am. Chem. Soc., 128 (2006) 398-399.

[21] L. Wang, Y. Xiao, W. M. Tian, L. Z. Deng. J. Am. Chem. Soc., 135 (2013) 2903-2906.

[22] M. A. Haidekker, T. P. Brady, D. Lichlyter, E. A. Theodorakis. Bioorg. Chem., 33 (2005) 415-425.

[23] F. Liu, T. Wu, J. F. Cao, S. Cui, Z. G. Yang, X. X. Qiang, S. G. Sun, F. L. Song, J. L. Fan, J. Y. Wang, X. J. Peng. Chem. Eur. J., 19 (2013) 1548-1553.

[24] Z. G. Yang, J. F. Cao, Y. X. He, J. H. Yang, T. Kim, X. J. Peng, J. S. Kim. Chem. Soc. Rev., 13 (2014) 4563-4601.

[25] Z. G. Yang, Y. X. He, J. H. Lee, N. Park, M. Suh, W. S. Chae, J. F. Cao, X. J. Peng, H. Jung, C. Kang, J. S. Kim. J. Am. Chem. Soc., 135 (2013) 9181-9185.

[26] F. Miao, W. J. Zhang, Y. M. Sun, R. Y. Zhang, Y. Liu, F. Q. Guo, G. F. Song, M. G. Tian, X. Q. Yu. Biosens. Bioelectron., 55 (2014) 423-429.

Scheme 1. The molecular structure and proposed mechanism of **MitoSN** for viscosity response.

Scheme 2. The synthesis routes of **MitoSN**.

Figure 1. (a) Changes of fluorescence spectra with variation of solution viscosity in water–glycerol system. (b) The fluorescence quantum yields of **MitoSN** with increasing solution viscosity. (c) The linear response between log (I/I_0) for **MitoSN** and log(viscosity) in the water/glycerol solvent.

Figure 2. (a) Colocalization fluorescence microscopy images of Hela cells treated with 10 μM **MitoSN** and Mito-Tracker Red. (b) Correlation plot of Mito-Tracker deep Red and **MitoSN** intensities; (c) Intensity profile of ROIs across Hela cells. Scale bar =20 μm.

Figure 3. Confocal microscopy images of Hela cells incubated with 10 μM **MitoSN** before and after treatment by CCCP and nystatin, respectively. Scale bar =20 μm.

Figure 4. Confocal fluorescence images of zebrafish (3-day-old) after being treated with **MitoSN** (10 μM) in water for 20 min (a), 1h (b) and 2 h (c). The scale bars: 100 μm.

Highlights

MitoSN possesses good hydrosoluble.

MitoSN exhibited ca. 35-fold fluorescence enhancement with the increasing viscosity.

MitoSN was sensitive to local viscosity and selectively stained mitochondria in living cells.

MitoSN displayed a significant luminescence in the whole body of zebrafish.

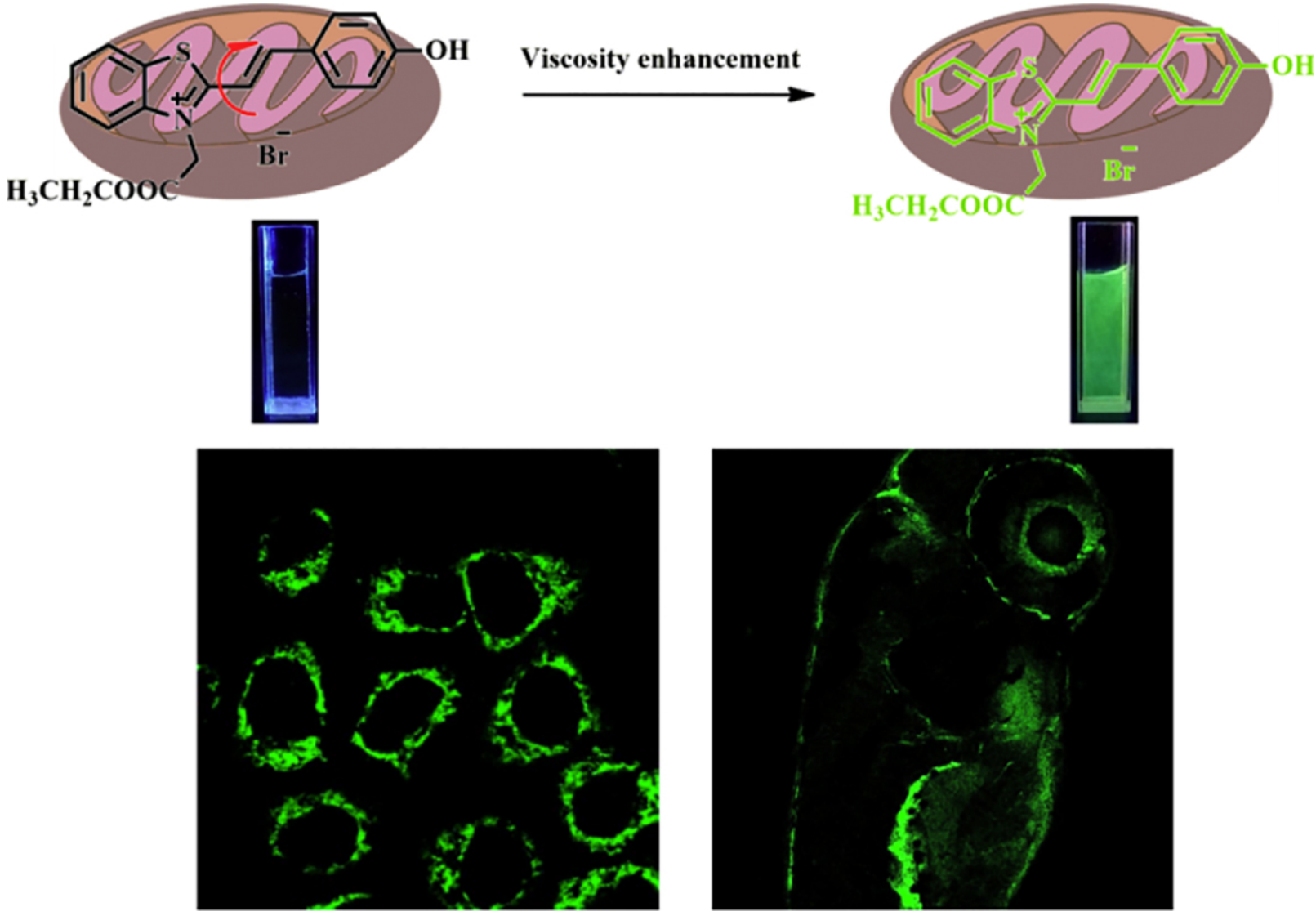

Graphics Abstract

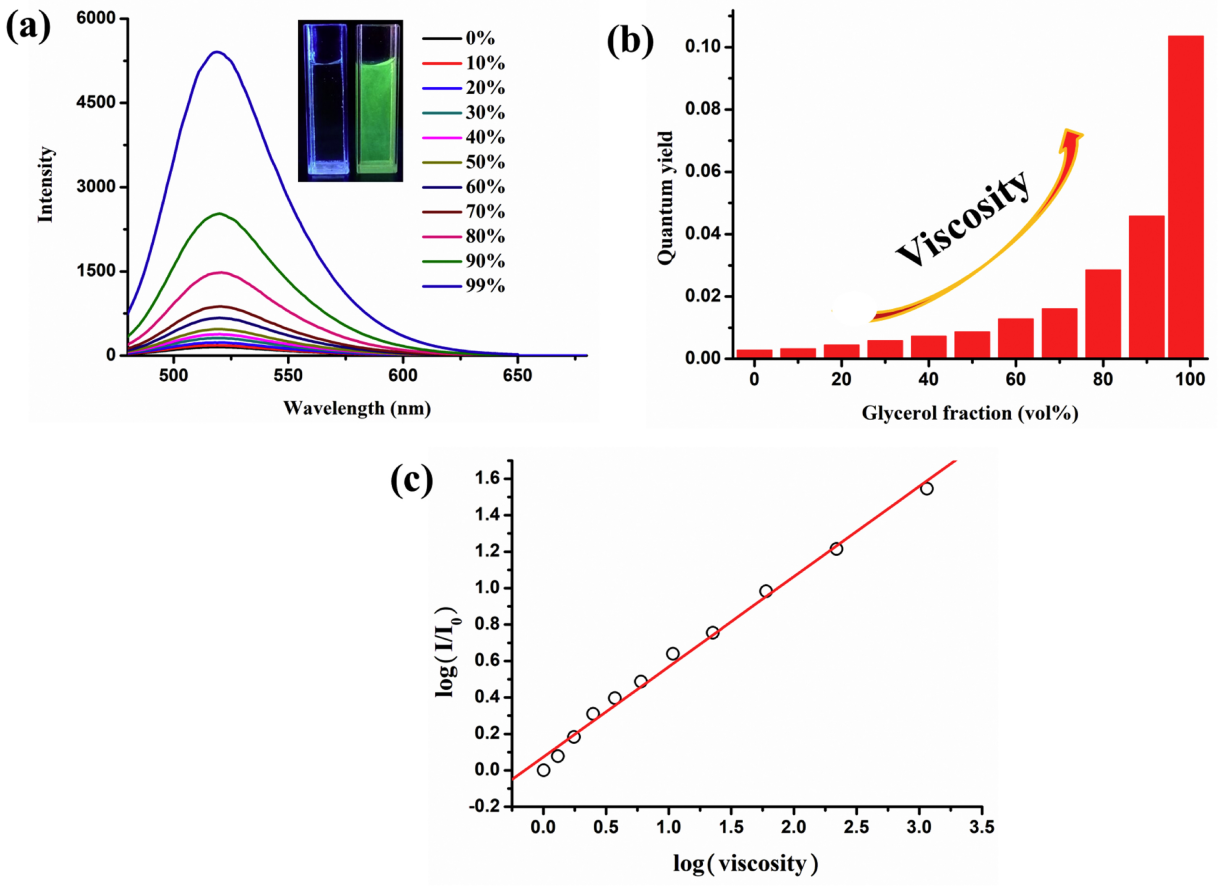
(a)
Intensity
Wavelength (nm)
0%
10%
20%
30%
40%
50%
60%
70%
80%
90%
99%
(b)
Quantum yield
Glycerol fraction (vol%)
Viscosity
(c)
log(I/I0)
log(viscosity)

Figure 1

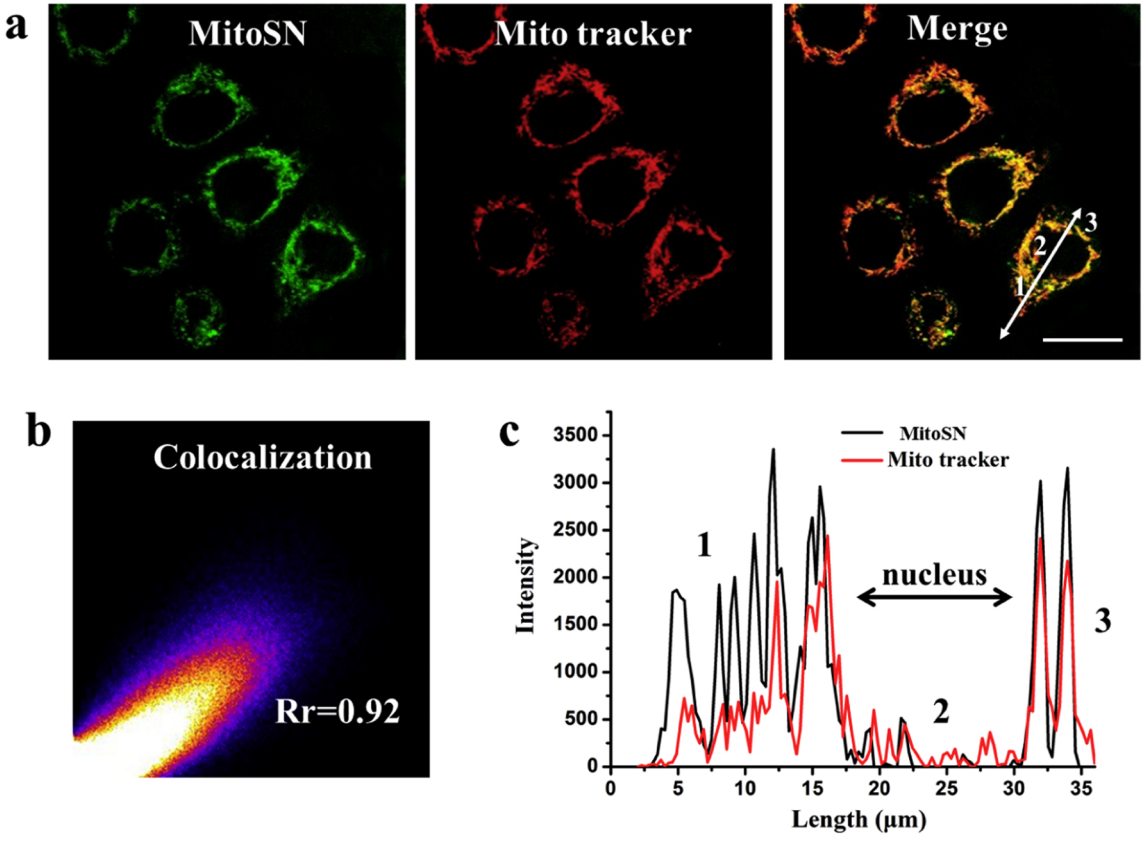
a
MitoSN
Mito tracker
Merge
1
2
3
b
Colocalization
Rr=0.92
c
MitoSN
Mito tracker
Intensity
Length (μm)
nucleus
1
2
3
0
500
1000
1500
2000
2500
3000
3500
0
5
10
15
20
25
30
35

Figure 2

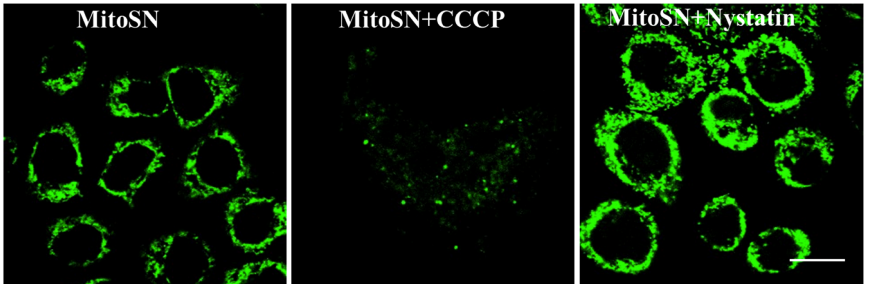
MitoSN
MitoSN+CCCP
MitoSN+Nystatin

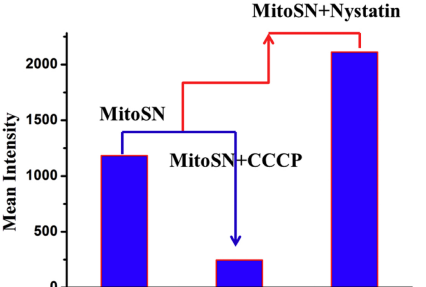
MitoSN+Nystatin
MitoSN
MitoSN+CCCP
Mean Intensity
2000
1500
1000
500
0

Figure 3

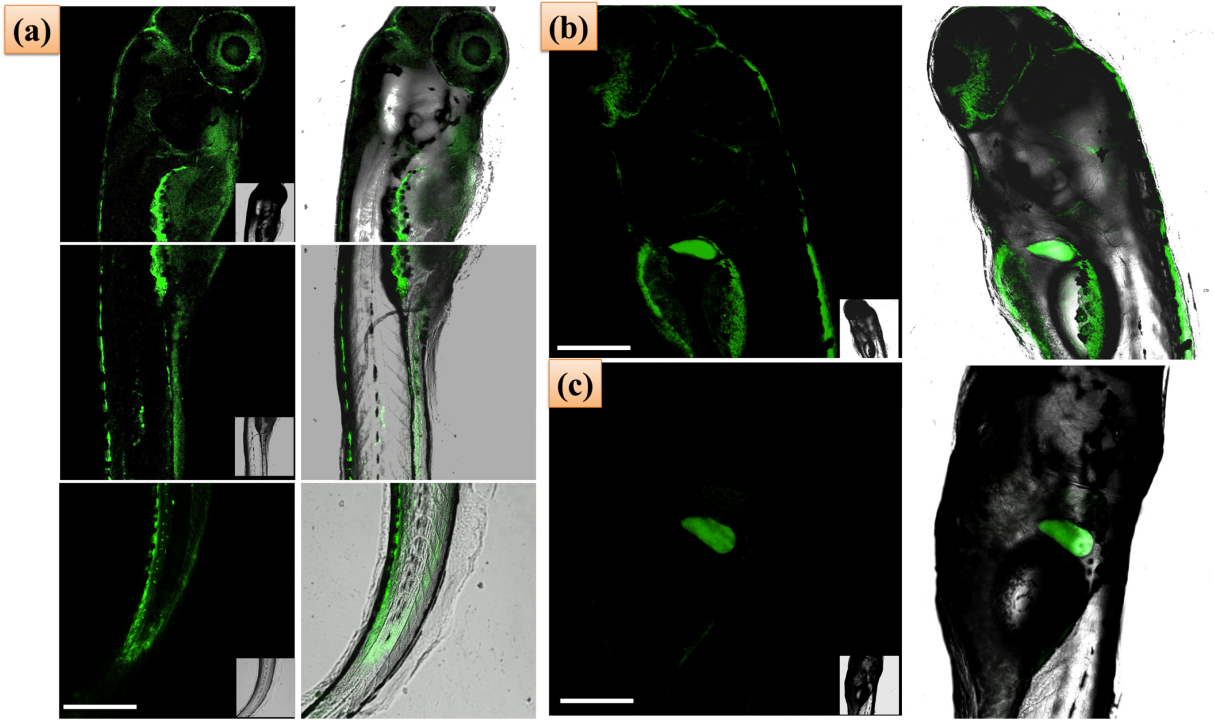

Figure 4